RASĀYAN *J. Chem.*
Vol. 19 | No. 4 | 2371-2378 | October-December | 2026
ISSN: 0974-1496 | e-ISSN: 0976-0083 | CODEN: RJCABP
http://www.rasayanjournal.com
http://www.rasayanjournal.co.in

FACILE SYNTHESIS OF COS_2/Mn COMPOSITE WITH ENHANCED ELECTROCATALYTIC ACTIVITY TOWARDS HYDROGEN EVOLUTION REACTION

C. K. Senthil Kumar[1], K. Saravanan[2],K. Margandan[3], A. Shalini[4]✉, and A. Priya[5]

[1]Department of Chemistry, Adhiparasakthi College of Engineering, Kalavai, Ranipet-632506, Tamil Nadu, India

[2]Department of Chemistry, Easwari Engineering College, Ramapuram, Chennai - 600089, Tamil Nadu, India

[3]Department of Chemistry, Erode Sengunthar Engineering College, Thudupathi, Erode-638057, Tamil Nadu, India

[4]Department of Chemistry, Faculty of Engineering and Technology, SRM Institute of Science and Technology, Ramapuram, Chennai- 600089, Tamil Nadu, India.

[5]Department of Chemistry, Aringar Anna Govt.Arts and Science College for Women, Ranipet-632513

✉Corresponding author: shaluchem28@gmail.com

ABSTRACT

To generate hydrogen fuel cells widely utilised, it is essential to design electrocatalysts that are both effective and economically viable for hydrogen evolution reaction applications. Here, we report a low-cost fabrication method for a CoS_2/Mn composite material that exhibits exceptional electrocatalytic activity for HER. The composite material was synthesised through a hydrothermal process, involving the combination of CoS_2/Mn composite by the wet impregnation method. The resulting material displayed a unique nanostructure, with CoS_2 nanoparticles uniformly dispersed on the Mn surface. The prepared nanocomposites were analysed using multiple characterisation techniques, including Fourier transform infrared spectroscopy (FTIR), powder X-ray diffraction (XRD), field emission scanning electron microscopy (FESEM), and transmission electron microscopy (TEM). We have examined the electrocatalytic activity of prepared CoS_2/Mn composites over the hydrogen evolution reaction. The CoS_2/Mn composites possess high electrocatalytic activity, with the smallest overpotential of 155 mV at 10 mA cm^{-2} and the lowest Tafel slope of 59 mV $dec^{-1}$with respect topure Mn and CoS_2. In addition to this, the optimizedCoS_2/Mn composite has a long-term stability in the acidic medium after 1000cycles. As a result, the fabricated CoS_2/Mn composite is used as an efficient electrocatalyst for HER application due to its cheap and Pt-free nature.

Keywords: Hydrogen Evolution Reaction (HER), Hydrothermal Method, Electrocatalysis, Cobalt Disulphide, and CoS_2/Mn Composite.

RASĀYAN*J. Chem.*, Vol. 19, No.4, 2026

INTRODUCTION

There is an immediate necessity to shift from fossil fuel–dependent energy storage and conversion technologies to sustainable and renewable energy sources. Acute require to transition from fossil fuel–based energy systems to sustainable alternatives has enhanced global research efforts toward clean and renewable energy technologies. Hydrogen, as a high-energy-density and carbon-neutral fuel, has become a key candidate for next-generation energy systems. In particular, electrochemical water splitting provides an environmentally benign and efficient route for hydrogen production when coupled with renewable energy sources.[1-4] However, the overall effectiveness of the processwasconsiderably restricted due to the sluggish kinetics of the hydrogen evolution reaction (HER), necessitating the synthesis of highly active, durable, and economically viable electrocatalysts.[5,22] Platinum (Pt)-based materials are widely regarded as benchmark HER catalysts due to their near-optimal, efficient hydrogen adsorption characteristics that promote high catalytic performance.[20,21]Despite their excellent performance, their high cost. High cost,

http://doi.org/10.31788/RJC.2026.1949922
This work is licensed under a CC BY 4.0 license.

lack of adequate attainability, and possibility of poisoning make it very hard to use them on a large scale.[6,7] As a result, the study of earth-abundant, non-noble metal catalysts has become a major focus of research in electrocatalysis.[2,8,22] Transition metal sulfides have gained substantial research interest among various alternatives owing to their adjustable electronic structures, inherent catalytic properties, and cost-effectiveness.[6,9,18] Cobalt disulfide (CoS_2), with a pyrite-type crystal structure and metallic conductivity, is known to be an efficient catalyst with significant potential for hydrogen evolution reaction (HER) applications.[7–10] The high density of electronic states near the Fermi level in CoS_2 makes it easy for electrons to move quickly and for hydrogen to stick to and come off the surface.[9,11] Even with these benefits, pure CoS_2 still has problems with limited active site exposure and poor hydrogen binding energy, which make it less effective as a catalyst.[10–12] To address these constraints, numerous approaches, including nanostructuring, defect engineering, and heteroatom incorporation, have been thoroughly examined.[18,25,26] Bimetallic engineering has been especially effective because adding a second metal can engineer the electronic characteristics, improve conductivity, and raise the density of functional active centres through synergistic interactions.[23,24,27] Manganese (Mn) has emerged as an effective dopant for modifying transition metal-based catalysts, primarily due to its multiple oxidation states and strong redox flexibility. Incorporation of Mn into catalytic systems can alter and reconfigure the electronic structure, enhance charge distribution, and reduce the hydrogen adsorption free energy, thereby enhancing reaction kinetics and overall catalytic efficiency.[14,15] Recent studies on Mn-containing heterostructures and composites have demonstrated enhanced electrocatalytic performance due to strong interfacial coupling and electronic interactions.[13–15] Despite these advances, systematic studies on Mn concentration-dependent tuning of CoS_2-based electrocatalysts remain limited. In particular, the correlation between Mn content, electronic structure modulation, and HER activity has not been fully established. Understanding this relationship is key to the fabrication of high-efficiency electrocatalysts. Herein, we report the controlled synthesis of CoS_2/Mn composites with varying Mn concentrations via a facile hydrothermal-assisted approach.[4,10,16] The incorporation of Mn into the CoS_2 matrix enables strong electronic coupling, enhanced charge transfer, and increased exposure of catalytically active sites. The optimised composite exhibits significantly improved HER performance, demonstrating the effectiveness of composition tuning in designing efficient and low-cost electrocatalysts.[17,23,28,29]

EXPERIMENTAL

Materials and Methods

Cobalt(II) chloride hexahydrate ($CoCl_2 \cdot 6H_2O$), thiourea (CH_4N_2S), cetyltrimethylammonium bromide (CTAB), and manganese acetate tetrahydrate ($Mn(CH_3COO)_2 \cdot 4H_2O$) were utilised as starting materials without any additional purification. Deionised water and ethanol served as the solvents for all synthesis procedures.

Synthesis of CoS_2Nanomaterial

We developed a CoS_2 nanomaterial with a basic and simple hydrothermal method. For the preparation of a homogeneous solution, Cobalt(II) chloride hexahydrate (4 mmol), thiourea (16 mmol), and cetyltrimethylammonium bromide (CTAB, 1 mmol) were mixed in 60 mL of deionised water and stirred with a magnet for 1 hour. Subsequently, following preparation, the reaction mixture was loaded into a Teflon-lined autoclave and heated at 180 °C for 12 h. After naturally cooling to room temperature, the obtained product was collected and repeatedly washed with deionised water and ethanol three times to eliminate residual impurities. Finally, the purified sample was dried in an oven at 80 °C for 3 h before further characterisation.

Synthesis of CoS_2/Mn Nanocomposite

The CoS_2/Mn nanocomposites were made using the same hydrothermal method. We added different amounts of manganese acetate tetrahydrate (0.1, 0.2, 0.3, and 0.4 mmol) to a beaker with the CoS_2 material that had already been made. The mixtures that came out of this were put through the same hydrothermal conditions as described above. The samples that were made were given the names pure CoS_2, CoS_2/Mn^{-1}, CoS_2/Mn-2, CoS_2/Mn-3, and CoS_2/Mn-4, which show that the amount of Mn in them is getting higher.

Characterization Techniques

We systematically characterised the synthesised materials' structural and morphological properties. We used X-ray diffraction (XRD, Rigaku D/Max-2500VB2/PC, Japan) to look at the phase purity and crystal structure. Scanning electron microscopy (SEM, Hitachi S-4700, Japan) was utilised to look at the surface morphology and microstructural features.

Electrochemical Measurements

Electrochemical analyseswere carried out using a standardthree-electrode configuration. Depending on the electrolyte employed, either an Ag/AgCl or Hg/HgO electrode was used asthe reference electrode, while a platinum wire was used as the counter electrode. For the Processingof the working electrode, 5 mg of the electrocatalyst was incorporated intoa solution containing 0.8 mL of deionised water, 0.2 mL of ethanol, and 30 μL of 5 wt% Nafion solution. Subsequently, the prepared suspension underwent ultrasonication for 60 min to ensure the formation of a homogeneous catalyst ink. Before catalyst deposition, the glassy carbon electrode (GCE, 5 mm diameter) was sequentially polished with alumina slurry and thoroughly washed several times with deionised water, followed by an ethanol rinse. Subsequently, 10 μL of the catalyst ink was drop-cast onto the cleaned GCE surface and Drying was carried out under ambient conditions without external heating. The catalyst loading on the electrode was maintained at 0.24 mg cm^{-2}.

RESULTS AND DISCUSSION

XRD Studies

The phase structure and crystallinity of the synthesised CoS_2/Mn composites with different Mn concentrations were studied using X-ray diffraction (XRD). The diffraction patterns of all samples show clear peaks that match the cubic pyrite structure of CoS_2(JCPDS No. 41-1471), evidencing the effective formation of the main phase. The well-defined diffraction peaks noted at 2θ values of about 10.8°, 12.3°, 16.2°, 32.8°, 36.3°, 49.8°, and 57.5° correspond to the (111), (200), (210), (211), (220), (311), and (222) crystal planes. The evident diffraction peaks are present across all samples, indicating that Mn incorporation does not significantly alter the fundamental crystal structure of CoS_2. At lower Mn concentrations, no additional impurity peaks are detected, suggesting that Mn ions are likely substituted into Co lattice sites. A slight shift in peak positions is observed, which may be ascribed to lattice distortion arising from the difference in ionic radii between Mn and Co, supporting the formation of a solid solution. With increasing Mn content, the diffraction peaks become broader and less intense, indicating a reduction in crystallite size and a decrease in crystallinity. This peak broadening may also result from increased lattice strain and defect formation induced by Mn doping. At higher Mn concentrations, the appearance of weak additional peaks suggests the formation of secondary phases, possibly related to Mn-containing compounds such as MnS. This indicates that excessive Mn incorporation leads to partial phase segregation rather than complete integration into the CoS_2 lattice. In summary, XRD findings suggest that Mn incorporation has a pronounced impact on the structural characteristics of CoS_2, including lattice distortion, reduced crystallite size, and the emergence of secondary phases at high concentrations.

Surface Morphology

Figure-2 depicts the FESEM analysis highlighting the structure of CoS_2 and CoS_2–Mn, revealing a well-defined three-dimensional flower-like morphology. The structure consists of densely packed nanosheets that radiate outward from a central core, forming a hierarchical microflower architecture. These nanosheets appear thin, wrinkled, and interconnected, creating a highly porous network. The integration of Mn into the CoS_2 framework greatly influences the nucleation and growth process, leading to a more uniform distribution of particles while preventing agglomeration. This results in a rough and porous surface with significantly enhanced surface area, thereby providing abundant electrochemically active sites. Such a distinctive morphology facilitates efficient electrolyte penetration and rapid charge transport, which is advantageous for electrocatalytic performance and sensing applications, particularly in cyclic voltammetry studies. Additionally, the FESEM micrographs reveal that the flower-like structures are evenly dispersed across the surface with negligible particle agglomeration, indicating effective control

over crystal nucleation and growth during the synthesis process. The self-assembled nanosheets form an interconnected porous framework containing numerous open channels, which can facilitate electrolyte infiltration and improve ion transport. The thin nanosheet petals expose a greater number of surface-active regions and edge sites, thereby increasing the availability of electrochemically accessible reaction centres. The incorporation of Mn contributes to the formation of a more uniform hierarchical architecture and helps preserve the integrity of the nanosheet assembly, resulting in improved structural stability. Such an interconnected porous network provides continuous pathways for both ion diffusion and electron transport, reducing charge transfer limitations at the electrode–electrolyte interface. The combination of the hierarchical flower-like morphology, rough surface texture, and porous nanosheet arrangement is expected to enhance the utilisation of active sites and promote faster electrochemical reaction kinetics. In addition, the robust microflower architecture can effectively accommodate structural changes during repeated electrochemical operation, thereby contributing to improved cycling durability. These morphological features demonstrate that Mn incorporation plays an important role in tailoring the surface architecture of CoS_2, making the CoS_2–Mn composite a promising electrode material for electrochemical sensing and other electrocatalytic applications.Transmission electron microscopy (TEM) indicates that clean CoS_2 has uniform nanostructures with a minor degree of agglomeration. When Mn is doped, the shape stays the same, but the dispersion improves, and the lattice is slightly distorted, showing that Mn has been successfully added to the CoS_2 framework. At medium levels of Mn, interconnected nanostructures with more defects and rougher surfaces are seen, which suggests that there are more active sites. But when there is more Mn, the structures come together to form flower-like shapes with blurred lattice fringes, which means they are less crystalline. Overall. the amount of Mn in CoS_2/Mn composites has an effect on their shape and structural integrity. A moderate amount of Mn gives the best dispersion and defect formation. In addition to this, the elemental composition for the synthesised composite materials was examined by the EDX elemental analysis. The pure CoS_2 contains Co and S elements only, whereas for and the composite material CoS/Mn contains Co, S and Mn elements only. This proved that no other impurities are present in this material. This shows that the composite was successfully fabricated.

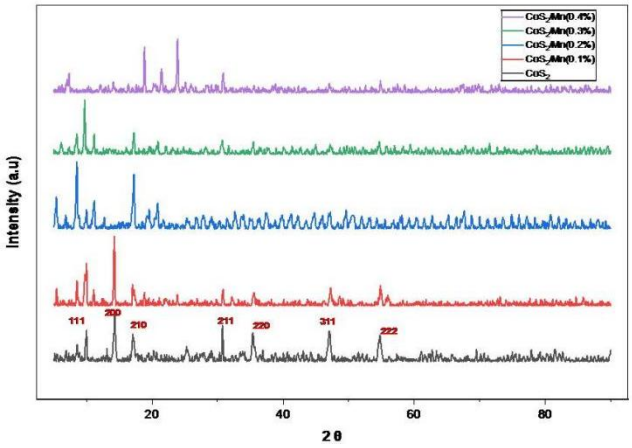


Fig.-1: XRD patterns of CoS_2, COS_2/Mn(0.1%), COS_2/Mn(0.2%), COS_2/Mn(0.3%) and COS_2/Mn(0.4%) (JCPDS No. 41-1471)

CoS_2/Mn Electrochemical Activity

Electrochemical measurement of the as prepared by using electrochemical analyzer CHE-608E three electrode system in 0.5M H_2SO_4 electrolyte and electrodes are Glassy carbon (GC) as an working electrode Silver / Silver chloride (Ag/AgCl) as an reference electrode Platinum (Pt) as an counter electrode, before using the working electrode polished and then coated by an drop cast coating method, precious that GC electrode washed with DI water after polish with micro polish powder then dried at room temperature 1 h, 2 mg of as synthesized material and 0.1 mL of Ethanol then 0.4 mL of DI water added in to reaction battle, was sonicated for 30 min, then link solution (5 mL) was coated on GC, coated electrode was tried at room temperature up to 1h.

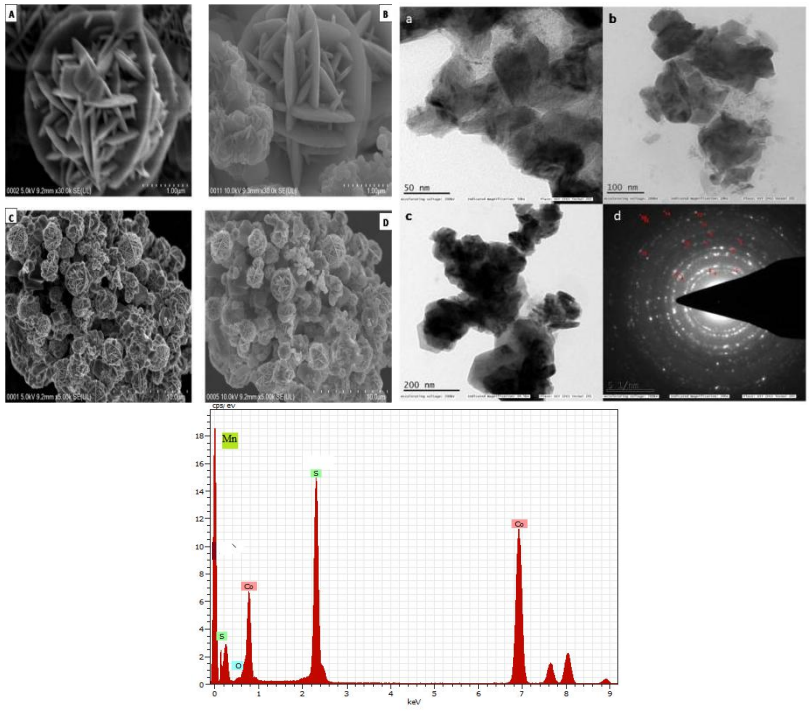


Fig.-2: Scanning Electron Microscope (FESEM) Imagery (A and B) at Low Magnification (C and D) at High Magnification, Transmission Electron Microscopy (HRTEM) Images at Low and High Magnification and EDAX For CoS2/Mn

Electrochemical analysis plots of the as-synthesised electrocatalyst are shown in Fig.-3. the polarization cure shown. The cathodic polarisation results of the various composite and pure materials are shown for HER activity. The overpotential (η_{10}) utilised to obtain an applied current density of 10 mA $cm^{-2}$is intended todetermine and contrast the HER efficiency of electrocatalysts since it is essential for making hydrogen from solar energy. Pure CoS required an overpotential of 0.43 V to reach 10 mA cm^{-2}, which is what it usually does. On the other hand, samples with Mn (Co_{1-x} Mn_xS, $x \neq 0$) showed much better performance. $Co_{0.94}Mn_{0.06}S$ showed a much lower overpotential of 0.216 V, which means that it had better hydrogen evolution activity in the low overpotential region. Tafel plots of the resulting The obtained materials are depicted in Fig.-4, plotting potentials versus current density again.

$$\eta = b \log (j) + a \quad [1]$$

Where *b* signifies the Tafel slope and *a* is the conversion current density. Tafel equation is a significant analytical and useful strategy to find out exactly what the HER mechanism accomplishes at the surface of the synthesised catalyst. The Tafel slope (b) remains constant regardless of the catalytic current, and hydrogen evolution follows distinct elementary pathways:

Initial discharge or Volmer step (120 mV/dec)

$$H_3O^+ + \text{electron} \rightarrow H_{ads} + H_2O \quad [2]$$

Heyrovsky step (40 mV/dec)

$$H_{ads} + H_3O^+ + \text{electron} \rightarrow H_2 + H_2O \quad [3]$$

Tafel step (30 mV/dec)

$$H_{ads} + H_{ads} \rightarrow H_2 \quad [4]$$

The electrocatalyst follows this mechanism is defined by a Tafel slope values. Synthesised $Co_{1-x}Mn_xS$ composites follow the Volmer mechanism to evaluate hydrogen evolution from an acid solution; the achieved Tafel slope value is 97 mV/dec for $Co_{0.94}Mn_{0.06}S$. The relatively low Tafel slope obtained for $Co_{0.94}Mn_{0.06}S$ further confirms the accelerated reaction kinetics during hydrogen evolution in an acidic electrolyte. The obtained value suggests that the initial proton adsorption (Volmer steps) proceeds efficiently, followed by rapid electron transfer at the catalyst –electrolyte interface. In addition to its

improved catalytic kinetics, the hierarchical morphology of the synthesised composite is expected to facilitate efficient electrolyte penetration and continuous exposure of catalytically active sites throughout the reaction. The interconnected nanostructure also promotes the rapid release of hydrogen bubbles from the electrode surface, minimising blockage of active sites and maintaining stable catalytic performance during prolonged operation. These combined structural and electronic advantages contribute to the excellent HER activity and demonstrate that Mn-modified cobalt sulfide is a promising electrocatalyst for sustainable hydrogen production under acidic conditions.

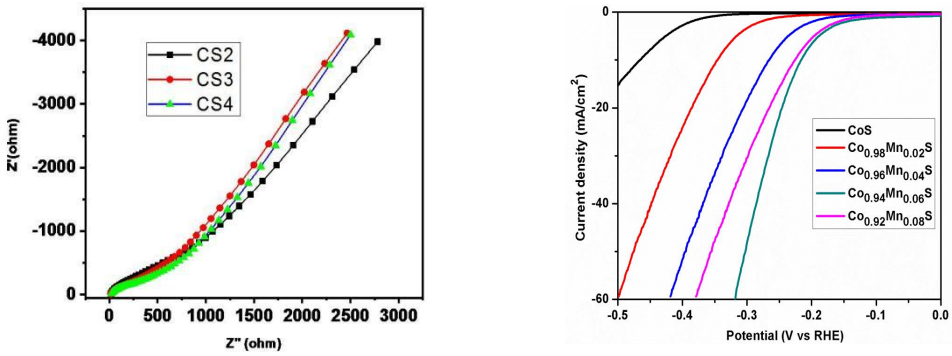


Fig.-3: Polarization Cures of Synthesized CoS and $Co_{1-x}Mn_xS$ at 5 mV/sScan Rate with 0.5 M H_2SO_4

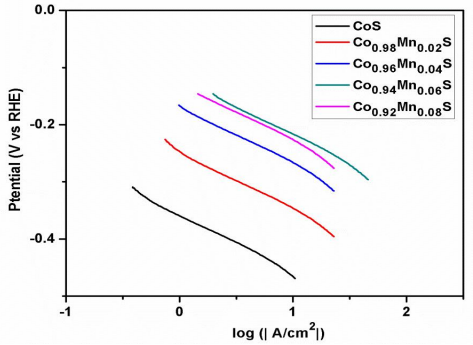


Fig.-4: Tafel Slope of the Synthesised Composites CoS and $Co_{1-x}Mn_xS$

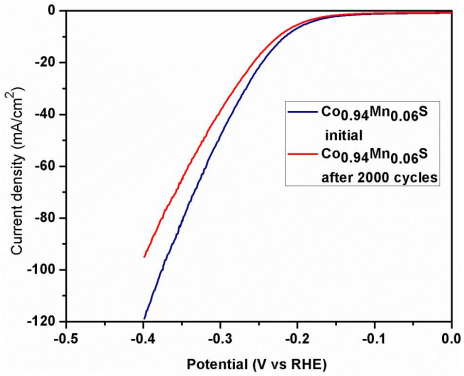


Fig.-5: Polarization Curves of $Co_{1-0.96}Mn_{0.6}S$ and

The electrochemical stability of detailed analysis was carried out on the synthesized electrocatalyst via cyclic voltammetry technique, here compared the initial and final polarization cures, the polarization allowed up to 2000 cycles from the first cycles, so the final polarized and initial polarized cures are shown Fig.-5. The comparison between these and the final cure gives slightly lower (7 %) activity recorded for $Co_{1-0.96}Mn_{0.6}S$; the prepared composites are very stable composites its giving enhanced electrochemical activity and higher stability towards the HER.

CONCLUSION

We made CoS_2/Mn composites by adding different amounts of Mn to a single pot and then heating it up. The CoS_2/Mn composites that were made have been evaluated as good electroactive catalysts employed in hydrogen production through HER in an acidic medium. The electrochemical analysis exhibited that the refined CoS_2/Mn composite delivered a current density of 10 mA cm^{-2} with an overpotential as low as 183 mV, a small Tafel slope of 73.95 mV dec^{-1}, and remarkable sustained cycling stability assessed againstpure Mo_2C. A greater efficiency was due to considering that there were a lot of many surface reactive centres, a large surface area, lower charge transfer resistance, and greater electrical conductivity. Those features were attained through the synergistic interaction between CoS_2 and Mn. Consequently, the CoS_2/Mn composite has been identified as an attractive replacement for Pt-based electrocatalysts in HER applications.

ACKNOWLEDGEMENTS

While writing this manuscript, AI-assisted tool(s) were used to make the language clearer and better. The authors thoroughly examined and edited the content, and they are completely responsible for the final published work.

CONFLICT OF INTERESTS

The authors declare that there is no conflict of interest.

AUTHOR CONTRIBUTIONS

The present work is related to *SDG-7: Affordable and Clean Energy*. All the authors contributed significantly to this manuscript, participated in reviewing/editing and approved the final draft for publication. The research profile of the authors can be verified from their ORCID ids, given below:

A.Shalini https://orcid.org/0000-0001-6059-5411
K.Saravanan https://orcid.org/0000-0003-0569-7508
K.Margandan https://orcid.org/0000-0002-5062-428X
C. K. Senthil Kumar https://orcid.org/0009-00092209-9295
A.Priya https://orcid.org/0009-0008-2114-1538

Open Access: This article is distributed under the terms of the Creative Commons Attribution 4.0 International License (http://creativecommons.org/licenses/by/4.0/), which permits unrestricted use, distribution, and reproduction in any medium, provided you give appropriate credit to the original author(s) and the source, provide a link to the Creative Commons license, and indicate if changes were made.
Cite this article as: C. K. Senthil Kumar *et al.*, *Rasayan J. Chem.*, 19(4), 2371-2378(2026), https://doi.org/10.31788/RJC.2026.1949922

REFERENCES

1. Z. W. Seh, J. Kibsgaard, C. F. Dickens, I. Chorkendorff, J. K. Nørskov, and T. F. Jaramillo, *Science*, **355(6321)**, eaad4998(2017), https://doi.org/10.1126/science.aad4998
2. I. Roger, M. A. Shipman, and M. D. Symes, *Nature Reviews Chemistry*, **1(1)**, 0003(2017), https://doi.org/10.1038/s41570-016-0003
3. J. Kibsgaard and T. F. Jaramillo, *Angewandte Chemie International Edition*, **53(52)**, 14433(2014), https://doi.org/10.1039/C5CS00151A
4. W. Rao, J. Shi, C. Yu, H. B. Zhao, and Y. Z. Wang, *Chemical Engineering Journal*, **424(4)**, 130556(2021), https://doi.org/10.1016/j.cej.2021.130556
5. Y. Zheng, Y. Jiao, A. Vasileff, and S. Z. Qiao, *Angewandte Chemie International Edition*, **57(26)**, 7568(2018), https://doi.org/10.1039/C3CS60468C
6. J. A. Turner, *Science*, **305(5686)**, 972(2004), https://doi.org/10.1039/C4EE00906C
7. M. Carmo, D. L. Fritz, J. Mergel, and D. Stolten, *International Journal of Hydrogen Energy*, **38(12)**, 4901(2013), https://doi.org/10.1021/nl400258t
8. X. Zou and Y. Zhang, *Chemical Society Reviews*, **44(15)**, 5148(2015), https://doi.org/10.1002/anie.201207111
9. J. A. Seabold and K. S. Choi, *Journal of the American Chemical Society*, **134(4)**, 2186(2012), https://doi.org/10.1002/ange.201200632

10. G. Näfe, M. A. López-Martínez, M. Dyballa, M. Hunger, Y. Traa, Th. Hirth, and E. Klemm, *Journal of Catalysis*, **329**, 413(2015), https://doi.org/10.1016/j.jcat.2015.05.017
11. J. Zhang, Y. Liu, C. Sun, and P. Xi, *ACS Energy Letters*, **3(4)**, 779(2018), https://doi.org/10.1021/acsenergylett.8b00066
12. L. Fang, Y. Zhang, Y. Guan, H. Zhang, S. Wang, and Y. Wang, *Journal of Materials Chemistry A*, **5(6)**, 2861(2017), https://doi.org/10.1039/c6ta10700a
13. J. Lee and J. Lee, *Korean Journal of Chemical Engineering*, **42(14)**, 3333(2025), https://doi.org/10.1007/s11814-025-00512-2
14. B. N. Darshan, A. Kareem, T. Maiyalagan, and V. E. Geo, *International Journal of Hydrogen Energy*, **46(27)**, 13952(2021), https://doi.org/10.1016/j.ijhydene.2020.09.151
15. S. Jafari and Z. Shaghaghi, *Scientific Reports*, **15(1)**, 4145(2025), https://doi.org/10.1038/s41598-025-87423-8
16. S. Parvaz et al., *Scientific Reports*, **14(1)**, 27622(2024), https://doi.org/10.1038/s41598-024-78870-w
17. S. Sekar et al., *Materials*, **18(16)**, 3775(2025), https://doi.org/10.3390/ma18163775
18. X. Liu, X. Shen, H. Li, P. Li, L. Luo, H. Fan, X. Feng, W. Chen, X. Ai, H. Yang, and Y. Cao, *Advanced Energy Materials*, **11(16)**, 2003905(2021), https://doi.org/10.1002/aenm.202003495
19. C. Duah, S. Jeon, R. E. Agbenyeke, J. Seo, C. G. Kim, Y. K. Lee, S. J. Lee, and W. Jung, *Journal of Materials Chemistry A*, **14(33)**, Advance Article(2026), https://doi.org/10.1039/D6TA01755J
20. J. K. Nørskov *et al.*, *Journal of The Electrochemical Society*, **152(3)**, J23(2005), https://doi.org/10.1149/1.1856988
21. G. Näfe and M.-A. López-Martínez, *Journal of Catalysis*, **329**, 413(2015), https://doi.org/10.1016/j.jcat.2015.05.017
22. Y. Li *et al.*, *Chemical Engineering Journal*, **430(4)**, 132896(2022), https://doi.org/10.1016/j.cej.2021.132896
23. J. Jiang *et al.*, *Advanced Functional Materials*, **32(11)**, 2109876(2022), https://doi.org/10.1002/adfm.202109876
24. J. Hou *et al.*, *Nano Energy*, **80**, 105504(2021), https://doi.org/10.1016/j.nanoen.2021.105504
25. Y. Xu *et al.*, *Energy Storage Materials*, **46**, 155(2022), https://doi.org/10.1016/j.ensm.2022.01.015
26. L. Zhang *et al.*, *Applied Catalysis B: Environmental*, **320**, 121948(2023), https://doi.org/10.1016/j.apcatb.2022.121948
27. X. Wang *et al.*, *Electrochimica Acta*, **389**, 138743(2021), https://doi.org/10.1016/j.electacta.2021.138743
28. H. Liu *et al.*, *Journal of Power Sources*, **520**, 230814(2022), https://doi.org/10.1016/j.jpowsour.2021.230814
29. Y. Cao *et al.*, *Renewable Energy*, **205**, 123(2023), https://doi.org/10.1016/j.renene.2023.01.045

[RJC-9922/2026]